Characteristics of Multiple Shock Wave/Turbulent Boundary-Layer Interactions in Rectangular Ducts

Bruce F. Carroll*
University of Florida, Gainesville, Florida
and
J. Craig Dutton†
University of Illinois at Urbana-Champaign, Urbana, Illinois

Multiple shock wave/turbulent boundary-layer interactions in a rectangular duct have been investigated using wall pressure measurements, surface oil flow visualization, spark schlieren photography, and laser Doppler velocimetry. Two undisturbed incoming Mach numbers were considered, Mach 2.45 and Mach 1.6. At Mach 2.45 the shock structure was a neutrally stable pattern of oblique shocks followed by repeated normal shocks with the level of flow confinement having only a small effect in the interaction. A large, three-dimensional separation region was observed. At Mach 1.6 the pattern consisted of a bifurcated normal shock followed by weaker, unbifurcated normal shocks. The boundary layer under the bifurcated shock was incipiently separated. In contrast to the Mach 2.45 case, the lower Mach number interaction was much steadier with the length of the interaction scaling directly with the level of flow confinement.

Nomenclature

h	= duct half-height (duct radius in axisymmetric geometries)
M	= Mach number
P	= pressure
Re	= Reynolds number
Re/m	= unit Reynolds number
X	= axial distance
δ	= boundary-layer thickness
δ^*	= displacement thickness
θ	= momentum thickness

Subscripts

u	= undisturbed value at start of interaction
0	= stagnation value prior to interaction

Introduction

MULTIPLE shock wave/turbulent boundary-layer interactions in constant or nearly constant area supersonic duct flows occur in a variety of devices including scramjet inlets, gas ejectors, and supersonic wind tunnels. For sufficiently high duct exit pressures, a multiple shock wave/turbulent boundary-layer interaction or shock train may form in the duct, causing a highly nonuniform and possibly unsteady flow at the duct exit. Lustwerk[1] has shown that flow confinement, as characterized by the ratio of the undisturbed boundary-layer thickness to the duct half-height (or radius in axisymmetric geometries) δ_u/h, significantly affects the interaction, leading to three types of shock systems: a single normal shock for small δ_u/h, a series of nearly normal shocks for moderate δ_u/h, and a series of oblique shocks for large δ_u/h. A brief discussion of the pertinent literature follows with a more complete literature review available in the report by Carroll and Dutton.[2]

Seddon,[3] Vidal et al.,[4] Kooi,[5] East,[6] and Delery[7] have all investigated the interaction of a single normal shock with a turbulent boundary layer under conditions of low confinement, i.e., small δ_u/h. In general, with undisturbed Mach numbers below 1.4, the boundary layer does not separate. At higher Mach numbers a bifurcated normal shock, with separation under the foot of the shock, is observed. A slip line is generated at the bifurcation point and extends downstream, static pressure and flow direction being matched across the slip line. After the interaction the flow is subsonic with the exception of a supersonic region or tongue[3] following the bifurcated portion of the shock. In an unconfined shock wave/turbulent boundary-layer interaction, the Mach number in the undisturbed core flow at the start of the interaction, M_u, and the Reynolds number based on undisturbed boundary-layer thickness, $Re_{\delta u}$, are the main governing parameters, with both the height of the bifurcation point above the wall and the tendency toward separation increasing as Mach number increases and as unit Reynolds number decreases.

Increasing levels of flow confinement significantly affect the interaction described. In contrast to the unconfined interaction, Mach number, M_u, and confinement parameter δ_u/h are the primary parameters affecting the confined interaction, as demonstrated by Merkli[8] and Mateer and Viegas,[9] while Reynolds number has a less pronounced influence. Mateer and Viegas[9] showed that increasing confinement (i.e., increasing δ_u/h) delays separation while Om et al.[10] observed that increased confinement tends to increase the size of the supersonic tongue. In a continuation of this work, Om and Childs[11] showed that further increases in δ_u/h for nearly constant Mach number and unit Reynolds number leads to a repeated normal shock pattern. Boundary-layer displacement thickness was found to increase rapidly through the first shock, then decrease slightly before increasing again across the second shock. This pattern was repeated through the entire interaction. The flow just outside the boundary layer stayed supersonic through the whole interaction, while the flow in the core region went subsonic after each shock, then reaccelerated to supersonic speeds before the next shock. At the end of the interaction the flow was still mixed supersonic/subsonic, with the supersonic portion isentropically decelerating to subsonic

Received May 31, 1988; presented as Paper 88-3805 at the 1st National Fluid Dynamics Congress, Cincinnati, OH, July 25-28, 1988; revision received Feb. 15, 1989.

*Assistant Professor, Department of Aerospace Engineering, Mechanics and Engineering Sciences. Member AIAA.

†Associate Professor, Department of Mechanical and Industrial Engineering. Member AIAA.

velocities. In Refs. 10 and 11, the Mach number ranged from 1.28 to 1.49 and confinement levels ranged from $\delta_u/h = 0.081$ to 0.198. Waltrup and Billig[12] investigated the interaction at higher Mach numbers and a range of Reynolds numbers and confinement levels. At Mach 1.53 a single normal shock was found. At Mach numbers from 1.68 to 2.97 a repeated oblique shock pattern was found. Similar results were reported by Ikui et al.,[13] who investigated shock trains at Mach numbers from 1.33 to 2.79. At $M_u = 1.33$ a single normal shock was observed. Mach numbers from 1.37 to 1.60 yielded multiple normal shocks, while Mach numbers from 1.86 to 2.79 caused multiple oblique shocks. When the Mach number exceeded 1.60 considerable flow asymmetry was observed. Shock motion was observed at all of these Mach numbers and was investigated using high-speed schlieren movies and high-speed wall pressure measurements. The amplitude of the shock oscillation increased with increasing Mach number. Ikui et al.[13] theorized that the shock motion is triggered by high-frequency pressure fluctuations in the incoming boundary layer while the frequencies of the shock motion are related to the resonance frequencies of the downstream subsonic duct flow. Terminal shock unsteadiness has also been observed in nominally steady ramjet inlet flows.[14] However, these results are not directly applicable to the current work since the subsonic flow downstream of the shock is subjected to a strong adverse pressure gradient in inlet geometries. Reynolds number effects on the shock structure are clearly seen by comparing the results of Mateer et al.[15] ($Re/m = 2.3 \times 10^7$, $M_u = 1.5$, $\delta_u/h = 0.202$), who found a single normal shock, to those of Om and Childs[11] ($Re/m = 4.9 \times 10^6$, $M_u = 1.49$, $\delta_u/h = 0.198$), who found a repeated shock system. Increasing the Reynolds number for essentially the same Mach number and confinement level causes the shock structure to shift from a multiple- to a single-shock system. The general effect of Mach number on the shock structure is that there is a tendency toward repeated shock systems as Mach number increases. The results of Waltrup and Billig[12] suggest that a single normal shock may not exist in high Mach number confined flows, even with small δ_u/h. However, the results of Cuffel and Back[16] with surface cooling indicate that a single normal shock can exist in a high Mach number flow with relatively large confinement ($M_u = 2.92$, $\delta_u/h = 0.348$).

Most of the previous investigations of shock train interactions under conditions of strong confinement have been limited to axisymmetric geometries, thus precluding the use of schlieren photography. Additionally, surface flow visualizations of the shock train interaction have not been reported. The current work fills this gap and helps clarify the differences between the structure and scaling of shock train interactions that occur at various Mach numbers and confinement levels. Several new qualitative features of the Mach 1.6 and 2.45 shock trains are also identified.

Experimental Setup

The experiments were performed in the Department of Mechanical and Industrial Engineering at the University of Illinois at Urbana-Champaign. A detailed description of the airflow facility is contained in the report by Carroll and Dutton.[2] High-pressure air is supplied by two compressors to a storage tank farm with an approximate volume of 150 m^3. At pressures below 760 kPa gage, a continuous flow rate of 1 kg/s is possible, higher flow rates being available in a blowdown mode. A 6-in. supply line connects the tank farm to a large axisymmetric plenum chamber with a flat circular faceplate designed to allow the connection of either axisymmetric or planar measurement sections. Flow leaving the attached measurement section is vented outside through a large silencing duct. A control valve/electronic controller is used to regulate the plenum pressure, which can be held constant automatically to within ± 0.7 kPa as the tank farm pressure varies.

A schematic is shown in Fig. 1 of the small-scale, planar, two-dimensional supersonic wind tunnel fabricated out of aluminum for use in this investigation. The wind tunnel, which has a constant width of 76.2 mm over the entire length, consists of a constant area stagnation chamber followed by a symmetric supersonic nozzle feeding directly into the rectangular test section. A symmetric nozzle is used such that the upper- and lower-wall boundary layers entering the test section have identical properties. At the exit of the test section a variable-area diffuser is mounted that can be adjusted to yield either a diverging or converging-diverging geometry. Optical access to the test section is provided by removable windows in the wind-tunnel side walls. Two interchangeable nozzle blocks were designed and built, one for Mach 2.45, the other for Mach 1.60.

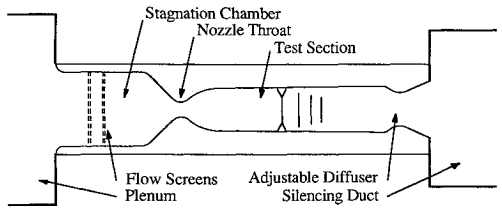

Fig. 1 Schematic of the small-scale planar supersonic wind tunnel, not to scale.

A description of the wind-tunnel configuration with the Mach 2.45 nozzle is given first. The upper and lower stagnation chamber, nozzle, and test section walls were each fabricated from a single piece of aluminum to avoid seams between sections. Two removable screens, each with 57.4% open area, are located in the rectangular stagnation chamber to help provide uniform mean and fluctuating velocity profiles. The stagnation chamber has a constant height of 101.6 mm. The nozzle has a throat height of 14.48 mm and an exit height of 38.1 mm. This nozzle, designed using the method of characteristics code of Carroll et al.,[17] yields a uniform Mach 2.45 flow based on wall static pressure measurements. The Mach 2.45 test section is 754 mm long and was originally made with a constant height of 38.1 mm. However, initial schlieren flow visualizations with these nozzle blocks revealed undesirable oscillatory movement of the shock train location on the order of a boundary-layer thickness in magnitude. In an effort to eliminate this shock motion, the test section walls were modified such that the upper and lower walls could be diverged by a variable angle of up to 1.25 deg each, with the divergence beginning at the nozzle exit. A boundary-layer trip was added to the converging part of the nozzle, and the variable area diffuser was used to isolate the test section from downstream fluctuations by forming a nearly sonic second throat. A series of schlieren visualizations with various test section divergence angles and diffuser geometries showed that the shock train unsteadiness was not visibly affected by the divergence angle or the presence of the boundary-layer trip. However, the second-throat diffuser did tend to make the mean shock location insensitive to relatively large variations in the plenum pressure on the order of 35–70 kPa. Additionally, the downstream silencing duct was temporarily removed, allowing the diffuser to vent directly into the room. Again, this had no visible effect on the shock steadiness. For the results presented in this paper, the test section divergence angle was held fixed at 0.25 deg for both the top and bottom walls to give a zero axial pressure gradient in the fully started test section. Static pressure taps were located along the centerline of the upper and lower test section walls with a minimum spacing between taps of 12.7 mm.

The Mach 1.6 nozzle was also designed to yield a uniform flow using the code of Carroll et al.[17] Based on wall pressure and laser Doppler velocimetry (LDV) measurements, the nozzle exit Mach number is slightly higher than 1.60. The nozzle throat height is 25.4 mm, and the exit height is 32.06 mm. The stagnation chamber has the same height as in the Mach 2.45 nozzle, and the two flow screens are again installed. Additional flow straightening in the stagnation chamber is pro-

vided through honeycomb installed ahead of the screens. The test section extends from the nozzle exit to 754 mm downstream. A fixed divergence angle of 0.13 deg was used for both the upper and lower test section walls in an effort to provide a zero pressure gradient in the fully started test section. As will be shown in the Results section, a small adverse pressure gradient resulted in the Mach 1.6 test section in spite of these efforts. Pressure taps were located only along the centerline of the upper test section wall, with a minimum spacing of 12.7 mm.

Two flow visualization techniques were used to investigate the qualitative features of the shock train phenomenon: schlieren photography and oil streak surface flow visualization. A standard Toepler schlieren arrangement was used. The light source was a Xenon model 457 1.4 μs duration light source that could be operated in either a single-spark mode or a stroboscopic mode for continuous viewing. A box camera, employing Polaroid Type 55 Positive/Negative sheet film (ASA 50) and 12-in. mirrors, was used for the Mach 2.45 case to give the maximum viewing area. With the Mach 1.6 case, the interaction was shorter, and 8-in. mirrors with a more convenient 35-mm mount and a Nikon F2 camera body using Kodak Pan-X film (ASA 32) were used. Oil streak surface flow visualization provided information concerning the separation and reattachment locations and the two dimensionality of the flow. The surface flow visualization was also used, in conjunction with soapy water applied to the external joints of the tunnel, to demonstrate that the test section was free of leaks. A mixture of gear oil and lampblack was either spread evenly over the test section surface or placed in discrete dots on the surface. The tunnel was then run for a sufficient amount of time to allow the surface streak pattern to set up. After shutting down the tunnel a sheet of tissue paper was carefully laid on the surface to absorb the resulting pattern. A photocopy of the tissue paper was then made to obtain a permanent record. While the tunnel was running, notes concerning the direction of the oil flow on the surface were taken. Appropriate arrows were later superimposed on the pattern to show these directions. The oil pattern was also observed during the tunnel shutdown process to insure that this transient did not significantly disturb the pattern.

A few cautionary words must be said concerning the interpretation of these flow visualizations. The schlieren and surface flow results are useful in studying the qualitative features of the flow. However, care must be taken not to draw excessively quantitative conclusions from these results. In particular, caution must be used in judging the velocity magnitudes through the interaction based solely on the schlieren photographs. Also, the surface flow results give a good indication of the flow directions at the surface, but should not be used to evaluate the flow too far away from the surface.

Measurements of the mean wall static pressure were made with two Pressure Systems Incorporated (PSI) model DP 6400T digital pressure transmitters. The first DP 6400T has 16 $\pm$100 kPa and 16 $\pm$200 kPa transducers, each having an estimated accuracy of $\pm$0.07 kPa. The second transmitter has 16 $\pm$310 kPa and 16 $\pm$690 kPa transducers, with an estimated accuracy of $\pm$0.17 kPa. The two pressure transmitters were connected to an HP 9000 host computer through a manual switching box such that a scan with the first transmitter could be immediately followed by a scan with the second transmitter. A scan of 32 ports took approximately 5 s. A complete scan using both transmitters took a total time of between 10 to 15 s. All data analysis and plotting was done on the HP 9000.

Velocity measurements for the Mach 1.6 shock train were made using a dual-beam, two-component, coincident LDV system described in detail in Refs. 2 and 18. LDV measurements were not made for the Mach 2.45 interaction since the higher level of shock unsteadiness in this case would have required conditional sampling to obtain meaningful results and the instrumentation for the conditional measurements was not available. The LDV system consists of a 5-W argon/ion laser and appropriate transmitting optics to generate two pairs of orthogonal beams. Frequency shifting at 40 MHz was used, as was 2.7x beam expansion. The resulting measurement volume had a diameter of 0.078 mm and an effective length of 1.8 mm. The receiving optics were oriented in a 10 deg off-axis forward-scatter arrangement. The LDV measurements are characterized as having a low burst density, i.e., a low probability of having more than one particle in the measurement volume at a time, and also as having low data density, i.e., the time between successive samples being large compared to the time scale of the turbulent fluctuations. The data acquisition system was able to process and transfer data at a rate much higher than the validated coincident data rate; hence, the LDV measurements are completely velocity biased. A two-dimensional velocity inverse weighting was used to correct for this velocity bias. Fringe bias effects were found to be negligible for this application. A complete discussion of the experimental error for the LDV measurements is given by Carroll and Dutton.[18]

Mach 2.45 Results

The experimental results for the Mach 2.45 shock train interaction are discussed here. Three cases, summarized in the first three lines of Table 1, are considered corresponding to three shock locations in the test section. For all three cases, the wind tunnel was operated at a nominal stagnation pressure of 310 kPa measured in the large plenum chamber. The adjustable diffuser was configured as a converging/diverging diffuser. By adjusting the size of the second throat, the shock train was positioned at the three desired locations. This series

Table 1 Experimental cases

δ_u, mm	δ_u, mm	δ_u^*, mm	δ_u/h	M_u	P_0, kPa	Re/m, $10^6 m^{-1}$
			Mach 2.45 cases			
3.0	—	—	0.15	2.45	307 $\pm$ 0.7	30.0
5.4	—	—	0.26	2.45	309 $\pm$ 0.7	30.0
7.3	—	—	0.35	2.45	309 $\pm$ 0.7	30.0
			Mach 1.6 cases			
1.3	0.09	0.22	0.08	1.63	206 $\pm$ 0.7	30.0
2.2	0.17	0.41	0.14	1.63	206 $\pm$ 0.7	30.0
4.4	0.34	0.80	0.27	1.62	206 $\pm$ 0.7	30.0
5.4	0.44	1.0	0.32	1.61	206 $\pm$ 0.7	30.0
6.7	0.56	1.3	0.40	1.60	206 $\pm$ 0.7	30.0
8.3	0.65	1.5	0.49	1.57	206 $\pm$ 0.7	30.0

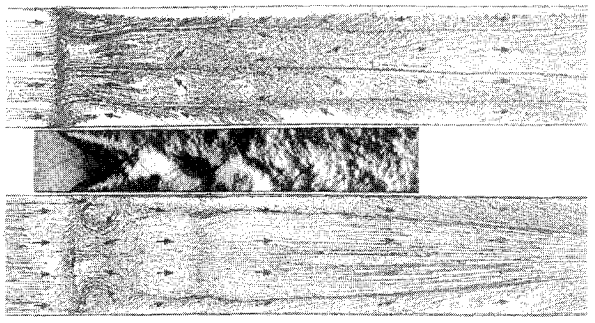

Fig. 2 Surface flow and schlieren; top: top wall surface flow, middle: side view schlieren, bottom: bottom wall surface flow, $M_u = 2.45$, $\delta_u/h = 0.15$.

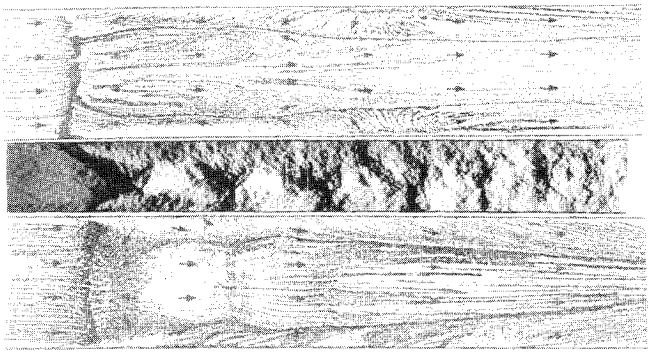

Fig. 3 Surface flow and schlieren; top: top wall surface flow, middle: side view schlieren, bottom: bottom wall surface flow, $M_u = 2.45$, $\delta_u/h = 0.26$.

of experiments is useful in investigating the effects of flow confinement as described by the ratio δ_u/h, with the Mach number and unit Reynolds number held constant. Reynolds number based on δ_u will change slightly as δ_u changes. For the Mach 2.45 case the undisturbed boundary-layer thicknesses δ_u, defined as the boundary-layer thicknesses at the start of the pressure rise, were estimated from the schlieren photographs. Similar estimates for the Mach 1.6 case were within 15% of the boundary-layer thickness determined from LDV measurements of the incoming boundary layer. The LDV measurements of the incoming boundary layer were not performed for the Mach 2.45 case.

Mach 2.45 Flow Visualizations

Typical schlieren and surface flow results for the Mach 2.45 interaction are given in Figs. 2 and 3. The top and bottom portions of the figures are the oil surface flow patterns of the top and bottom test section walls, respectively. Between these is shown the schlieren, to scale with the surface flow, viewed through the window in the tunnel side wall. As discussed later, the surface flow for the third case could not be performed due to flow unsteadiness. In Fig. 3 the schlieren picture shown consists of two photographs joined together. The entire shock train could not be photographed at once due to the limited field of view of the schlieren apparatus. In both figures the schlieren was set up with a vertical knife edge such that accelerations show as light regions and decelerations as dark regions and the flow is from left to right.

Consider first the case with a confinement level of $\delta_u/h = 0.15$ (Fig. 2). In the schlieren photograph, weak Mach waves can be seen in the incoming flow. These were generated by the growing boundary layer in the nozzle and by any slight imperfections in the nozzle contour. The first shock in the shock train is an asymmetric oblique shock pattern. The top leading oblique shock originates in the upper wall boundary layer upstream of the location where the bottom leading oblique shock originates in the lower wall boundary layer. The two leading shocks cross below the centerline. After crossing, the two shocks terminate a fair distance from the nozzle wall, indicating a substantial subsonic region near the wall. Following the first oblique shock pattern, the flow reaccelerates. One cannot determine from the schlieren photograph if the flow in this core region is totally supersonic or if the reacceleration occurs from subsonic initial velocities. However, based on the incoming Mach number and the measured shock wave angles, the initial shocks appear to be weak oblique shocks. The second and later shocks are not as well defined but appear to be nearly normal in character near the lower wall and tend to "lie" along the lower wall without extending all the way to the upper wall. In the shock pattern shown the shock train is described as being "attached" to the lower wall, even though boundary-layer separation is present on both walls. This pattern was neutrally stable, with the shock system sometimes being attached to the lower wall and sometimes attached to the upper wall, occasionally flipping from one wall to the other during the course of a run. A large amplification in the scale of the turbulence structure is observed going through the interaction, and the boundary layer is seen to thicken substantially through the interaction.

Turning attention to the surface flow pattern for this case, one observes two highly different patterns on the top and bottom walls. This is not surprising in light of the asymmetric shock pattern described. On the top wall a fairly straight separation line occurs slightly upstream of the separation on the bottom wall. Following the separation on the top wall is a large, three-dimensional reverse flow region. The flow reattaches first near the center of the tunnel and heads downstream, with some of the flow closer to the side walls turning and heading back upstream. The flow reattaches near the side walls last. This type of reattachment could be described as a U-shaped reattachment with the open part of the U facing downstream. Substantial corner effects are seen on the upper wall, with the flow near the corner heading away from the side wall. Following complete reattachment, the flow in the central portion of the tunnel is again fairly two dimensional. On the bottom wall the separation line is again nearly straight. The separation region is much smaller and the reattachment line is only slightly curved. Distinct vortex patterns exist in the separation region near the side walls. Again, corner effects are seen after reattachment that grow in size at a faster rate on the bottom wall than on the top wall, with only the middle third of the flow being two-dimensional at the end of the picture. In a study of supersonic flow through a square duct without shocks, Davis et al.[19] observed a pair of counter-rotating secondary flow cells centered about the corner bisector. Such a phenomenon could explain the corner effect observed here.

Moving to the second case with $\delta_u/h = 0.26$ (Fig. 3), the results are similar to those with $\delta_u/h = 0.15$. The shock system now tends to flip, from top-wall shock attachment to bottom-wall attachment, or vice versa, more often. The case of bottom wall shock train attachment is shown. In the schlieren picture a small amount of oil can be seen on the window, appearing as small streaks on the glass. The schlieren picture is very similar to the $\delta_u/h = 0.15$ case with the asymmetric oblique initial shock, followed by a series of shocks that are more normal in character. The overall length of the interaction has not noticeably increased. The top-wall surface flow again shows a nearly straight separation line with a U-shaped reattachment. However, the flow now reattaches closer to the separation line. The reattachment near the wall is clearer in this picture, showing a star pattern at the wall. The flow following reattachment is again fairly two dimensional on the top wall with appreciable corner effects. On the bottom wall the size and shape of the separation region are very similar to the $\delta_u/h = 0.15$ case. The second shock is seen to cause a necking in of the corner flow and an accumulation of oil under the shock. The third shock causes a similar but weaker effect. This necking in is also observed in the $\delta_u/h = 0.15$ case but is not as

noticeable. The washed-out region between the first and second shock is presumed to be caused by the reacceleration of the flow following the first shock. Efforts to improve the recorded pattern by placing additional oil in this washed out area and rerunning the experiment were unsuccessful. The oil quickly left this region before the other features of the surface flow could set up. Again, a large increase in the corner effect is seen on the bottom wall following the interaction.

At $\delta_u/h = 0.35$ the shock train would not stay attached to a single wall long enough for the surface flow pattern to develop. Therefore, only the schlieren visualization was obtained but is not included here. The flow pattern was more symmetric, with both the first and second shocks being oblique shocks. The later shocks still tend to attach to either the upper or lower wall in a neutrally stable manner. The length of the interaction is about the same as in the two preceding cases.

In all three cases substantial flow unsteadiness was present. The following qualitative discussion of shock unsteadiness emphasizes aspects of the problem that deserve further investigation. The wall pressure measurements were mean in nature and correspondingly incapable of resolving high-frequency pressure fluctuations. Therefore, the unsteadiness phenomenon was only studied visually with the stroboscopic schlieren. Two types of unsteadiness were observed. The first was the neutrally stable shock pattern, which tends to flip from one wall to the other at random times. This phenomenon was more pronounced with the shock train located near the end of the duct. This could be due to the increased flow confinement or to a change in the characteristics of the subsonic flow between the shock train and the converging/diverging diffuser. This first type of unsteadiness has not been previously reported and is a phenomenon that requires further study. Instabilities of this type would have a highly adverse effect on scramjet inlet operation. The second type of unsteadiness was in the form of higher-frequency shock motion aligned with the flow direction. The amplitude of this motion was on the order of an undisturbed boundary-layer thickness. Ikui et al.[13] observed this type of unsteadiness and postulated that this motion was controlled by resonance of the subsonic flow after the duct. The findings of McLafferty et al.[20] substantiate this conclusion. As was discussed earlier, the second-throat diffuser in this study isolated the shock train from downstream disturbances in the silencing duct such that resonance could occur only in the test section.

Mach 2.45 Pressure Mesurements

Wall static pressure measurements were obtained for the three Mach 2.45 cases summarized in Table 1, with the results presented in Fig. 4. In Fig. 4 the shock system is attached to the bottom wall for all cases and the pressure is measured on the top wall. The wall static pressure P has been normalized by the stagnation pressure before the interaction P_0, and the pressure traces have been shifted such that the downstream distance is measured from the start of the interaction. The ideal value of P/P_0 following a normal shock at Mach 2.45 is 0.432. The maximum measured values of P/P_0 after the shock train interaction are 0.374, 0.350, and 0.318 for $\delta_u/h = 0.15$, 0.26, and 0.35, respectively. Thus, the pressure recovery through the shock train ranges from 86.5 to 73.4% of the ideal normal shock value. This last value of 73.4% may be slightly low as the pressure recovery may not have been completed before the exit of the duct in this case. A comparison of the traces shows that the initial pressure rise is very similar for all three cases, with the steep initial pressure rise followed by a pressure plateau and a region of more gradual downstream pressure recovery. This agrees with the findings of Waltrup and Billig[12] in their investigation of shock trains in circular ducts. The similarity between cases is also consistent with the flow visualizations. As was noted in the schlieren results, the structure of the shock system, which causes the pressure rise, does not change appreciably as δ_u/h increases. The top-wall surface flow patterns change somewhat from case to case, but would not be expected to have a great effect on the wall

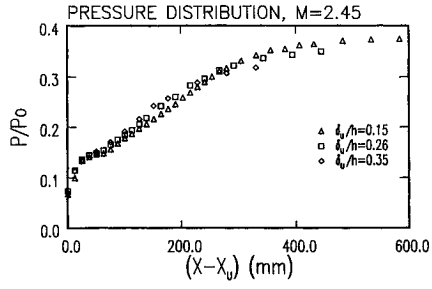

Fig. 4 Dimensionless wall static pressure distributions shifted to begin at the start of the pressure rise, $M_u = 2.45$.

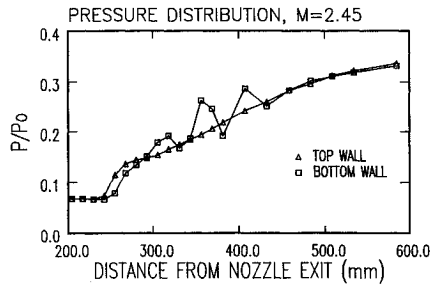

Fig. 5 Top- and bottom-wall static pressure distributions, $M_u = 2.45$, $\delta_u/h = 0.26$.

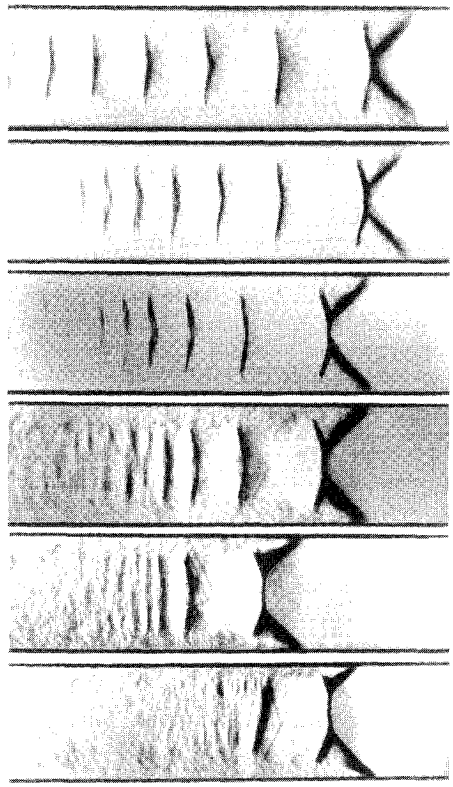

Fig. 6 Schlieren, vertical knife edge, $M_u = 1.6$; from top to bottom $\delta_u/h = 0.08, 0.14, 0.27, 0.32, 0.40, 0.49$.

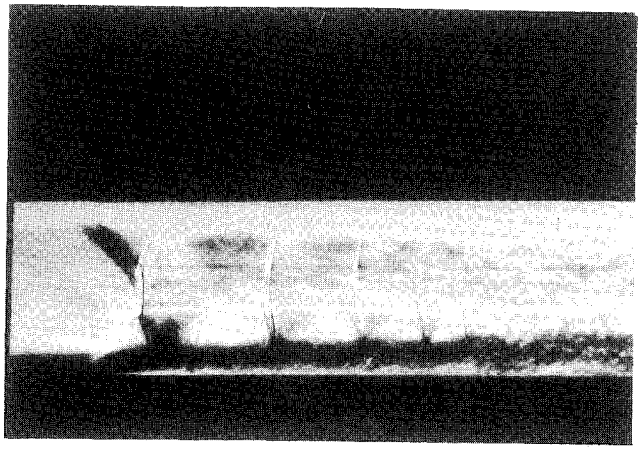

Fig. 7 Schlieren, horizontal knife edge, $M_u = 1.6$, $\delta_u/h = 0.32$.

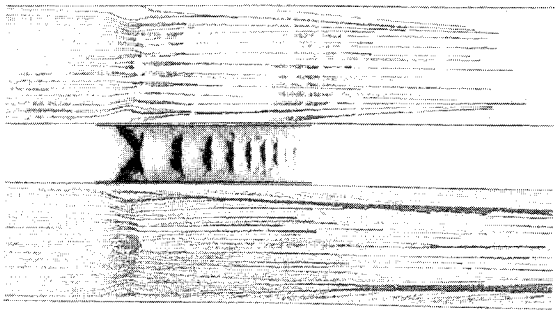

Fig. 8 Surface flow and schlieren; top: top wall surface flow, middle: side view schlieren, bottom: bottom wall surface flow, $M_u = 1.6$, $\delta_u/h = 0.40$.

pressure. As is discussed later, the relative insensitivity of the Mach 2.45 oblique shock train wall pressure distribution to the level of flow confinement is in direct contrast to the Mach 1.6 normal shock train interactions strong dependence on the confinement level.

A previously unreported aspect of the Mach 2.45 shock train is illustrated in Fig. 5, where the top- and bottom-wall pressure distributions for the $\delta_u/h = 0.26$ case are shown. In this case the shock system is attached to the bottom wall. (The bottom-wall measurement was actually obtained using the pressure taps on the top wall but with the shock attached to the top wall. This was done to take advantage of the finer pressure tap spacing on the top wall.) The smooth pressure distribution occurs on the top wall, where the larger separation region is present. The jagged pressure trace on the bottom wall was caused by the normal shocks lying very close to the surface. The initial pressure rise starts on the top wall first since the upper oblique shock slightly leads the bottom oblique shock. The top- and bottom-wall pressure traces eventually coincide near the end of the interaction. Differences between the two profiles occur only in the middle of the shock train, where normal shocks lie along one wall.

Mach 1.6 Results

Six cases are considered for the Mach 1.6 interaction. A summary of these cases is given in Table 1. The stagnation pressure was held at a nominal value of 207 kPa for this set of experiments, and the shock location was varied by adjusting the throat gap on the adjustable diffuser, configured as a symmetric converging/diverging second-throat diffuser. The test section was built with a fixed constant divergence angle of 0.13 deg on each side or a 0.26-deg total divergence angle. This divergence angle was expected to provide a neutral pressure gradient in the undisturbed boundary layer, but a small adverse pressure gradient is present. Therefore, the Mach number is only approximately constant in this series of experiments, the unit Reynolds number is held constant, and the flow confinement parameter δ_u/h is varied. The undisturbed boundary-layer thickness δ_u, momentum thickness θ_u, and displacement thickness δ_u^* were determined from LDV measurements of the incoming boundary layers for each confinement level. A complete description of the procedures used to determine these undisturbed boundary-layer parameters is given in Ref. 2. In the following section the schlieren and LDV results are discussed first. The surface flow visualizations and mean wall static pressure measurements are then described. Detailed LDV measurements through the shock train were only performed for the $\delta_u/h = 0.32$ confinement level. The surface flow visualizations for each case were so similar that only the surface flow results for $\delta_u/h = 0.40$ are presented.

Mach 1.6 Flow Visualizations and LDV Result

The schlieren results are presented in Figs. 6–8 with the flow from left to right. The knife edge is vertical in Figs. 6 and 8, with decelerations showing as dark areas and accelerations as light regions. A horizontal knife edge was used for Fig. 7. In Fig. 6 the schlieren was adjusted to a lower sensitivity to view the shape of the shock waves in the center of the duct without interference from the side wall shock wave/boundary-layer interaction. The top picture shows the shock positioned near the nozzle exit, where the boundary layer is thinnest. Proceeding from top to bottom, the shock is progressively further from the nozzle exit and the boundary layer is correspondingly thicker. The shock train is very symmetric in all cases except for $\delta_u/h = 0.08$, where a slight asymmetry occurs. In all cases an increase in the boundary-layer thickness and an amplification of the turbulence scales is observed going through the interaction. The first shock is always bifurcated, while the following "secondary" shocks are not. The bifurcated shock consists of a leading oblique shock, a nearly normal outer shock, and a trailing oblique shock with the three intersecting at the bifurcation point. A slip line, visible in Fig. 7, is generated at the bifurcation point and extends downstream. A diamond-shaped reion of flow reacceleration, especially visible in Fig. 8, exists immediately behind the outer normal shock and trailing oblique shock. The schlierens suggest that a weak compression wave may exist at the downstream border of the diamond-shaped reacceleration region. A similar compression wave, reflected from the interaction of the trailing shock with the boundary layer, was also observed by Chriss et al.[21] Downstream of the diamond region the darker shading indicates that the flow is only weakly accelerating or even decelerating. The size and shape of the first shock and the diamond region remains approximately the same as δ_u/h increases, with the height of the bifurcation point above the wall increasing only slightly. The distance from the end of the diamond to the second shock, and consequently the spacing between the first and second shock, increases as confinement levels increase.

The shocks following the first shock, termed secondary shocks, are similar to each other but different in character than the first shock. The secondary shocks are unbifurcated. The outer region is nearly normal, being concave facing downstream, as opposed to the first shock, in which the normal portion was concave facing upstream. An inflection point in the shock shape is seen to occur where the slip line from the bifurcation point of the first shock crosses the secondary shocks. This is clearly visible in Fig. 7. A diamond-shaped reacceleration region follows each secondary shock but is not as well defined as the first diamond. Within a single shock train the spacing between successive downstream shocks decreases. As confinement increases, the number of secondary shocks, the spacing between respective shocks in each shock train, and the overall length of the interaction increase.

The steadiness of the interaction was observed with the schlieren light source in the continuous viewing mode. These observations agreed with the findings of Ikui et al.[13] The mean shock train location was fixed with only very small amplitude oscillations in the leading shock's streamwise location. Each successive secondary shock showed motion of increasing amplitude. The last few secondary shocks in each shock train were very weak and displayed small-scale movement less than an undisturbed boundary-layer thickness δ_u in amplitude. In contrast to the higher Mach number case, the Mach 1.6 shock train is symmetric, and no noticeable shock motion was observed in the direction normal to the wall.

A Mach number contour plot generated from the LDV data taken along the midplane of the tunnel is presented in Fig. 9 for the $\delta_u/h = 0.3$ case. The measurements were concentrated in the regions just prior to the first shock, between the first and second shocks, and between the second and third shocks. The spacing between traverses in the later regions of the shock train were too large to resolve the details of the flow following the third shock in the system. However, the measurements do resolve the flow redevelopment downstream of the shock train. These Mach number contour plots display several features of the flow which are seen in the schlieren photographs. The heavy solid lines are sonic lines ($M = 1.0$), the light solid lines are supersonic, and the light dashed lines are subsonic. A subsonic pocket is seen to exist immediately downstream of the first and second shocks. This pocket corresponds roughly to the lightly shaded diamond shaped region in the schlieren pictures. Downstream of this diamond region a nearly constant Mach number area exists prior to the next shock in the system. Thus, speculation just raised in the discussion of the schlieren results about the existence of this nearly constant velocity region is confirmed. Existence of the slip line in the flow is also evidenced in the LDV measurements. This slip line begins at the bifurcation point of the first shock and extends downstream, causing the notch in the contours midway between the centerline and the sonic line in the boundary layers. A large growth in the thickness of the boundary layers is also caused by the interaction. The LDV measurements indicate that the boundary layer never separates, i.e., reversed mean flow is never measured. However, immediately below the bifucated first shock, a substantial number of the instantaneous velocity samples had reverse velocities, indicating that the boundary layer is probably best described as being incipiently separated by the first shock. Downstream of the interaction, a region of supersonic flow near the boundary-layer edge persists for several duct heights. This supersonic tongue is quite similar to that observed downstream of a single normal shock/turbulent boundary-layer interaction.[3]

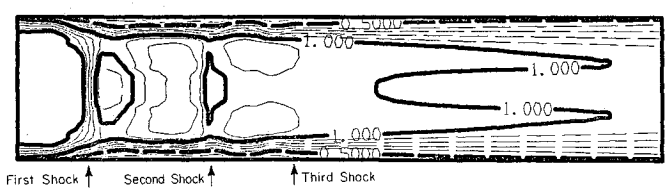

Fig. 9 Dimensionless wall static pressure distributions, shifted to begin at the start of the pressure rise, $M_u = 1.6$.

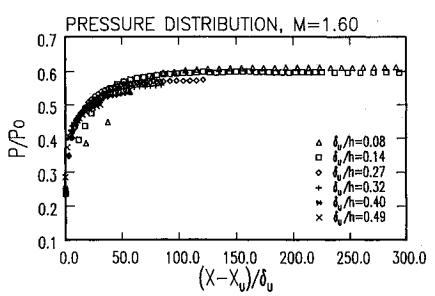

Fig. 10 Mach number contour plot from LDV measurements, $M_u = 1.6$, $\delta_u/h = 0.32$.

The surface flow visualization for $\delta_u/h = 0.40$ and Mach 1.6 is shown in Fig. 8. As was done with the Mach 2.45 case, the top and bottom test section wall surface flow oil streak patterns are shown above and below the side view schlieren photograph. This figure is representative of all of the surface flow results at Mach 1.6. On the top wall discrete drops of oil were placed on the duct wall. On the bottom wall the entire surface was coated with oil. A small accumulation of oil is seen below the first shock. This is caused by the incipiently separated condition detected with the LDV measurements. Under conditions of low confinement, a Mach 1.6 normal shock/turbulent boundary-layer interaction would be strongly separated. As was mentioned in the Introduction, decreased separation size is a characteristic of strongly confined interactions. A slightly larger oil accumulation is seen near the corner and along the centerline. The secondary shocks do not separate the flow. A corner effect develops after the side wall separation under the first shock and continues to grow with downstream distance. The flow after the first shock appears to flow out of the corner, possibly due to some type of rotating secondary flow in the corner.[19] At the end of the picture the middle 50% of the flow is still two-dimensional. The surface flow visualizations indicate a higher level of two-dimensionality than indicated from the LDV measurements. A limited number of spanwise LDV traverses showed that the mean streamwise velocity in the incoming boundary layer was uniform to within 0.25% over the middle 50% of the tunnel. Just downstream of the first shock the side wall boundary layer caused a greater spanwise variation in the flow. The spanwise uniformity was better than 2.6% over the middle 25% of the tunnel and was better than 9.4% over the middle 50% of the tunnel. Downstream of the shock train the spanwise nonuniformities diminished. At 37 undisturbed boundary-layer thicknesses downstream of the start of the interaction, the streamwise velocity was uniform to within 0.8% over the middle 25% of the tunnel and to within 6.2% over the middle 50% of the tunnel.

Mach 1.6 Wall Pressure Measurements

The wall static pressure measurements for the six Mach 1.6 cases in Table 1 are presented in Fig. 10. The wall static pressure P has been normalized by the upstream stagnation pressure P_0. When the downstream distance is measured from the start of the interaction and is normalized by the undisturbed boundary-layer thickness at the start of the interaction, δ_u, the Mach 1.6 wall pressure data collapses fairly well to a single curve, with the exception of the $\delta_u/h = 0.08$ case. The reason for this exception is unclear but could be due to the slight asymmetry of the shock train for this case. The Mach 2.45 results were plotted in the same dimensionless manner as Fig. 10 but failed to collapse to a single curve, the reason being that at the lower Mach number the spacing between shocks in the shock train and the number of shocks in the shock train are strongly linked to the level of confinement, while at Mach 2.45 this dependence on flow confinement is not observed. This result demonstrates a fundamental difference in the pressure recovery process for the strongly separated Mach 2.45 shock train and the incipiently separated Mach 1.6 case. As the Mach 1.6 shock train is moved away from the nozzle exit to a downstream location with higher confinement, the length of the pressure rise increases and the overall pressure recovery decreases. The ideal pressure recovery through a normal shock at Mach 1.6 is $P/P_0 = 0.663$. The pressure recovery through the shock train interaction was $P/P_0 = 0.609$, 0.596, 0.574, 0.536, and 0.500 or 91.9, 89.9, 86.6, 84.1, 80.8, and 73.4% of the ideal value for $\delta_u/h = 0.08$, 0.14, 0.27, 0.32, 0.40, and 0.49, respectively. The pressure recovery has been completed by the duct exit for the first four cases, possibly for

the fifth case, but not for the sixth case, where the shock train is closest to the exit. The strong confinement effects cause a less than ideal pressure recovery across the shock train.

Conclusions

An experimental investigation of the multiple shock wave/turbulent boundary-layer interaction in a rectangular duct has been performed for incoming Mach numbers of 2.45 and 1.6. The length of the interaction and the tendency toward a repeated oblique, rather than normal, shock system increases with Mach number. At Mach 2.45, the shock train was an asymmetric, oblique shock system, with the surface flow and wall static pressure distributions exhibiting different characteristics on the upper and lower duct walls. Surface flow visualization revealed a large separated region characterized by a two-dimensional separation and a three-dimensional reattachment. The separated regions display very different flow patterns on the opposing walls due to the asymmetry of the oblique shock train. Two modes of unsteadiness in the oblique shock train were observed. The first was a high-frequency streamwise oscillation. The second, which has received little attention in the past, is a low-frequency transverse oscillation related to the neutrally stable, asymmetric character of the shock pattern. As the level of confinement increased, the length of the Mach 2.45 interaction did not change appreciably; i.e., the length of the higher Mach number, oblique shock systems does not appear to scale with the level of confinement. In contrast, the Mach 1.6 shock train was a much steadier, symmetric, normal shock system. The number of shocks in the shock system and the length of the interaction were found to scale directly with the level of confinement. A small, incipiently separated region was observed under the first, bifurcated shock in the system. The secondary, unbifurcated shocks did not separate the boundary layer.

Acknowledgments

This work was funded in part by an Office of Naval Research Graduate Fellowship for B. F. Carroll and by ONR Research Contract N00014-85K-0665 monitored by S. G. Lekoudis. Additional support was provided by the Department of Mechanical and Industrial Engineering, University of Illinois at Urbana-Champaign, and by the Aero Propulsion Laboratory, Wright-Patterson Air Force Base, with A. S. Nejad as technical monitor.

References

[1]Lustwerk, F., "The Influence of Boundary Layer on the 'Normal' Shock Configuration," Meteor. Rept. 61, Massachusetts Institute of Technology Guided Missiles Program, Cambridge, MA., Sept. 1950.

[2]Carroll, B. F., and Dutton, J. C., "A Numerical and Experimental Investigation of Multiple Shock Wave/Turbulent Boundary Layer Interactions in a Rectangular Duct," Department of Mechanical and Industrial Engineering, Univ. of Illinois at Urbana-Champaign, Urbana, IL, Rept. UILU-ENG-88-4015, Aug. 1988.

[3]Seddon, J., "The Flow Produced by Interaction of a Turbulent Boundary Layer with a Normal Shock of Strength Sufficient to Cause Separation," British Aeronautical Research Council, London, R&M 3502, March 1960.

[4]Vidal, R. J., Wittliff, C. E., Catlin, P. A., and Sheen, B. H., "Reynolds Number Effects on the Shock Wave-Turbulent Boundary Layer Interaction at Transonic Speeds," AIAA Paper 73-661, July 1973.

[5]Kooi, J. W., "Experiment on Transonic Shock-Wave Boundary Layer Interaction," (NATO) AGARD CP 168, May 1975.

[6]East, L. F., "The Application of a Laser Anemometer to the Investigation of Shock-Wave Boundary Layer Interactions," (NATO) AGARD CP 193, May 1976.

[7]Delery, J. M., "Experimental Investigation of Turbulence Properties in Transonic Shock/Boundary Layer Interactions," *AIAA Journal*, Vol. 21, No. 2, 1983, pp. 180–185.

[8]Merkli, P. E., "Pressure Recovery in Rectangular Constant Area Supersonic Diffusers," *AIAA Journal*, Vol. 14, No. 2, 1976, pp. 168–172.

[9]Mateer, G. G., and Viegas, J. R., "Effect of Mach and Reynolds Numbers on a Normal Shock-Wave/Turbulent Boundary-Layer Interaction," AIAA Paper 79-1502, July 1979.

[10]Om, D., Viegas, J. R., and Childs, M. E., "Transonic Shock-Wave/Turbulent Boundary Layer Interactions in a Circular Duct," *AIAA Journal*, Vol. 23, No. 5, 1985, pp. 707–714; also AIAA Paper 82-0990, 1982.

[11]Om, D., and Childs, M. E., "Multiple Transonic Shock-Wave/Tubulent Boundary Layer Interaction in a Circular Duct," *AIAA Journal*, Vol. 23, No. 10, 1985, pp. 1506–1511; also AIAA Paper 83-1744, 1983.

[12]Waltrup, P. J. and Billig, F. S., "Structure of Shock Waves in Cylindrical Ducts," *AIAA Journal*, Vol. 11, No. 10, 1973, pp. 1404–1408.

[13]Ikui, T., Matsuo, K., Nagai, M., and Honjo, M., "Oscillation Phenomena of Pseudo-Shock Waves," *Bulletin of the JSME*, Vol. 17, No. 112, 1974, pp. 1278–1285.

[14]Sajben, M., Bogar, T. J., and Kroutil, J. C., "Experimental Study of Flows in a Two-Dimensional Inlet Model," *Journal of Propulsion and Power*, Vol. 1, No. 2, 1985, pp. 109–117.

[15]Mateer, G. G., Brosh, A., and Viegas, J. R., "A Normal Shock-Wave Turbulent Boundary-Layer Interaction at Transonic Speeds," AIAA Paper 76-161, Jan. 1976.

[16]Cuffel, R. F., and Back, L. H., "Flow and Heat Transfer Measurements in a Pseudo-Shock Region with Surface Cooling," *AIAA Journal*, Vol. 14, No. 12, 1976, pp. 1716–1722.

[17]Carroll, B. F., Dutton, J. C., and Addy, A. L., "NOZCS2: A Computer Program for the Design of Continuous Slope Supersonic Nozzles," Dept. of Mechanical and Industrial Engineering, Univ. of Illinois at Urbana-Champaign, Urbana, IL, Rept. UILU ENG-86-4007, Aug. 1986.

[18]Carroll, B. F. and Dutton, J. C., "An LDV Investigation of a Multiple Normal Shock Wave/Turbulent Boundary Layer Interaction," AIAA Paper 89-0355, Jan. 1989.

[19]Davis, D. O., Gessner, F. B., and Kerlick, G. D., "Exerimental and Numerical Investigation of Supersonic Flow Through a Square Duct," *AIAA Journal*, Vol. 24, No. 9, 1986, pp. 1505–1515; also AIAA Paper 85-1622, 1985.

[20]McLafferty, G. H., Krasnoff, E. L., Ranard, E. D., Rose, W. G., and Vergara, R. D., "Investigation of Turbojet Inlet Design Parameters," United Aircraft Corp., Research Dept., East Hartford, CT, Rept. R-0790-13, Dec. 1955, pp. 17–58.

[21]Chriss, R. M., Keith, T. G., Jr., Hingst, W. R., Strazisar, A. J., and Porro, A. R., "An LDA Investigation of Three-Dimensional Normal Shock-Boundary Layer Interactions in a Corner," AIAA Paper 87-1369, June 1987.